Improvement of Peroxygenase Activity by Relocation of a Catalytic Histidine within the Active Site of Horseradish Peroxidase

Marina I. Savenkova, Jane M. Kuo, and Paul R. Ortiz de Montellano*

Department of Pharmaceutical Chemistry, School of Pharmacy, University of California, San Francisco, California 94143-0446

Received October 17, 1997; Revised Manuscript Received May 13, 1998

ABSTRACT: To examine the role of Arg38 in the peroxidative and peroxygenative activity of horseradish peroxidase (HRP), we have expressed the R38A, R38H, and R38H/H42V mutants. The R38A HRP mutant gives a normal compound **I** species with H_2O_2 that is reduced by ferrocyanide to the ferric state without the detectable formation of a compound **II** species. In the case of the R38H and R38H/H42V mutants, compound **I** itself is only detected by stopped flow methods. The rates of compound **I** formation at 4 °C are 8.0×10^4, 1.3×10^6, and 1.6×10^3 M^{-1} s^{-1} for the R38A, R38H, and R38H/H42V mutants, respectively. The R38A, R38H, and R38H/H42V mutants oxidize guaiacol 10-, 2-, and 55-fold, respectively, more slowly than the wild-type enzyme and oxidize ABTS 6-, 3-, and 32-fold more slowly than the wild-type enzyme. The apparent k_{cat}/K_m values for thioanisole sulfoxidation and styrene epoxidation indicate that the reaction efficiencies of the R38H and wild-type enzymes are comparable. However, the R38A and R38H/H42V mutants are 190- and 1400-fold more efficient as sulfoxidation catalysts, and 25- and 26-fold more efficient as styrene epoxidation catalysts, respectively, than the wild-type enzyme. Thus, even though Arg38 plays a role in the formation and stabilization of compounds **I** and **II**, its replacement by other residues can be used to improve peroxygenative catalysis.

The catalytic turnover of horseradish peroxidase (HRP)[1] is initiated by reversible reaction of the enzyme with H_2O_2 to form compound **0**, a ferric peroxide ($Fe{\cdot}H_2O_2$) complex, that is subsequently converted to compound **I**. Two oxidation equivalents are stored in compound **I**, one as a ferryl ($Fe^{IV}{=}O$) species and the second as a porphyrin radical cation ($P^{\bullet+}$) (*1*−*4*). The activation of other hemoprotein peroxidases by H_2O_2 is similar, although in some instances (e.g., cytochrome *c* peroxidase, CcP), one of the oxidation equivalents is stored as a protein rather than as a porphyrin radical (*5*). The peroxidase catalytic cycle is completed by sequential transfer of two electrons to the activated enzyme. The first of these electrons quenches the porphyrin (or protein) radical to give compound **II**, and the second reduces the ferryl species to regenerate the resting ferric enzyme (*1*). With few exceptions, the two electrons come from separate substrate molecules, resulting in the oxidation of each to a free radical. The reduction of compound **I** to compound **II** is often rapid in the native enzyme compared to the reduction of compound **II**, so that compound **II** is commonly observed in the steady-state turnover of the enzyme (*6*).

A histidine and an arginine are found distal to the heme in the active sites of the structurally characterized peroxidases (Figure 1) (*7*−*12*). The presence of these two residues in CcP, the first peroxidase for which a crystal structure was obtained (*7*), led Poulos and Kraut to postulate that they catalyze the reaction of the enzyme with H_2O_2 to produce compound **I** (*13*). This proposal is supported for CcP by the demonstration that mutation of the distal histidine (His52) to an alanine decreases compound **I** formation by a factor of 10^5 (*14*). Mutation of the distal arginine (Arg48) in CcP to an alanine has a smaller impact but still decreases the rate of compound **I** formation by a factor of 10^2 (*15*). Recent studies have demonstrated that mutation of the corresponding residues in HRP also has a severe impact on peroxidase activity. Mutation of His42, the distal histidine, to an alanine or a leucine decreases the rate of compound **I** formation by

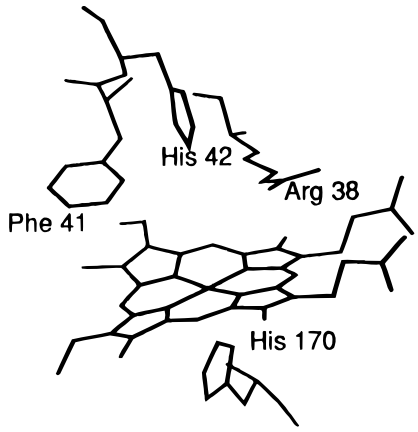

FIGURE 1: Model of the active site of HRP based on the crystal structure of the active site of peanut peroxidase (*11*). The Phe41, His42, and Arg38 residues that restrict access to the ferryl oxygen are shown, as is the proximal ligand His170. The heme group is shown edge-on from the perspective of the putative substrate access channel.

* To whom correspondence should be addressed. FAX: (415) 502-4728. E-mail: ortiz@cgl.ucsf.edu.

† This work was supported by National Institutes of Health Grant GM32488.

[1] Abbreviations: heme, iron protoporphyrin IX regardless of oxidation and ligation state; HRP, horseradish peroxidase isozyme *c*; hHRP, polyhistidine-tagged recombinant horseradish peroxidase; R38A and R38H hHRP, the Arg38 → Ala and His mutants of hHRP, respectively; R38H/H42V hHRP, the Arg38 → His, His42 → Val double mutant of hHRP; ABTS, 2,2′-azino-bis(3-ethylbenzothiazoline-6-sulfonic acid).

S0006-2960(97)02578-6 CCC: $15.00 © 1998 American Chemical Society
Published on Web 07/09/1998

a factor of $\sim 10^6$ (*16*, *17*). Mutations of Arg38, the distal arginine in HRP, have also been reported: (a) replacement of Arg38 by a lysine produces a protein that is hexacoordinate and has low activity (*18*, *19*) and (b) replacement of Arg38 by a leucine gives an active protein for which the rate of compound **I** formation is decreased by a factor of 10^3 (*17*, *20*). The distal histidine and arginine thus appear to have comparable roles in HRP and CcP.

HRP and related enzymes normally do not catalyze peroxygenation reactions in which two-electron reduction of compound **I** is coupled to the transfer of the ferryl oxygen to a substrate. The only well-established exception to this rule is the sulfoxidation of thioanisoles and related sulfur compounds, for which ferryl oxygen transfer has been demonstrated by ^{18}O-labeling studies (*21*, *22*). The almost negligible activity of peroxidases as peroxygenases may stem from steric sequestration of the ferryl species in a manner that interferes with its interaction with potential substrates (*2*, *23*, *24*). Restricted access to the ferryl species does not interfere with peroxidase catalysis because it can occur by electron transfer to the heme edge rather than by transfer directly to the ferryl species (*2*, *16*, *23*). Support for this hypothesis is provided by the finding that mutation of the distal histidine in HRP to an alanine or valine, which drastically decreases compound **I** formation but increases access to the ferryl oxygen, results in a 13- and 9-fold increase, respectively, in the rate of thioanisole sulfoxidation (*25*). Substantial increases are also observed in the rates of styrene epoxidation. In an effort to improve the peroxygenase activity of the His42 mutants, we have sought to restore the high rate of compound **I** formation without decreasing access to the ferryl oxygen. We previously demonstrated for H42A hHRP that its rate of compound **I** formation and the rates of two of its peroxygenase activities are increased by adding exogenous imidazoles (*16*) or by displacing the catalytic histidine to position 41 in the active site (i.e., as in the F41H/H42A double mutant) (*26*).

In HRP, Arg38, like His42, forms part of the protein barrier that restricts the interaction of substrates with the ferryl oxygen (Figure 1). The data on the Arg mutants of CcP (*15*) and the R38L mutant of HRP (*17*, *20*) suggest that replacement of the distal arginine by a noncatalytic residue has a much smaller impact on the rate of compound **I** formation than comparable replacement of the distal histidine. We have therefore investigated the effect of replacing Arg38 by an alanine or a histidine on the peroxidase and peroxygenase activities of HRP and have examined the catalytic consequences of combining the R38H and H42V mutations.

EXPERIMENTAL PROCEDURES

Materials. Native HRP and bovine serum albumin were from Boehringer Mannheim (Indianapolis, IN). Restriction enzymes were purchased from Boehringer Mannheim, New England Biolabs (Beverly, MA) and Gibco BRL (Grand Island, NY). Hemin, 30% H_2O_2, thioanisole, styrene, and ABTS were obtained from Aldrich (St. Louis, MO). Guaiacol was from Sigma (Milwaukee, WI). H_2O_2 was quantitated by its absorbance at 240 nm using the extinction coefficient 39.4 M^{-1} cm^{-1} (*27*). For enzyme quantitation, the Soret absorbance of the HRP mutants was taken to be the same as that of native HRP (ϵ = 102 000 M^{-1} cm^{-1}).

Tissue Culture. Spodoptera frugiperda (Sf9) cells were maintained in spinner flasks at 27 °C (75 rpm) in Hink's TNM-FH medium supplemented with Grace's medium (JRH Biosciences) containing 10% heat-inactivated, 0.2-μm-filtered fetal calf serum (UCSF Cell Culture facility). *Trichoplusia ni* cells (InVitrogen) were maintained in suspension in Sf900-II SFM medium (Gibco BRL) in a rotary shaker incubator at 27 °C (130 rpm).

Site-Directed Mutagenesis, Subcloning, and Production of Recombinant Virus. Mutant hHRP genes were constructed by cassette mutagenesis. Double-stranded DNA cassettes bearing the proper mutation and sticky ends for *Sac*I and *Nhe*I restriction sites (coding for amino acids 26−60) were synthesized and inserted into the pUC-HRP construct cut with *Sac*I and *Nhe*I. Proper orientation of the insert was checked, and the mutant HRP gene was cut from the pUC vector at the *Eco*RI sites and inserted into the pAcGP67B vector bearing the leader sequence and a 10-histidine tag (*25*). Subcloning was accomplished in *Escherichia coli* Dh5α competent cells. The Sf9 insect cells were then infected with the hHRP-pAcGP67B construct using the Baculovirus Gold system (InVitrogen). After one round of plaque purification, the virus was transfected into Sf9 insect cells using a multiplicity of infection of 4−6.

For protein expression, 1 L of *T. ni* insect cells at a concentration of 1.7−2.5 million/mL was infected with the stock solution of the virus at a multiplicity of infection of 1−5. The virus was added together with heme (final concentration 0.3 mg/mL) and 10 mL Pen/Strep solution (100 000 μg streptomycin and 100 000 units penicillin G). For R38H/H42V hHRP expression, 0.01 mM imidazole was also added. Cultures were incubated for 64−68 h at 27−29 °C in a rotary shaker at 130 rpm, after which the supernatant was collected and the protein was purified.

Protein Purification. The supernatant obtained by centrifugation of the cells (2000*g*, 10 min) was concentrated and ultrafiltered at ~25 °C with an Amicon spiral-wound cartridge concentrator model CH2PRS (S1Y10, 10 000 MW cutoff spiral membrane) to a final volume of 150−200 mL. The buffer was 20 mM Na_2HPO_4 (pH 8.0) containing 500 mM NaCl. After centrifugation (12000*g*, 30 min) of the ultrafiltrate, the supernatant was stirred with 7.5−10 mL of Ni(II)-NTA (InVitrogen) at 4 °C for 1.5−2 h. The resin was then collected in a 1.5-cm diameter column support, and the resulting column was washed with 1 mL/min of the same buffer until the eluent was clear. The resin was then washed with 20 mM Na_2HPO_4 (pH 6.0) buffer containing 500 mM NaCl, followed successively by washes with the same buffer containing 0.1 M and finally 1.0 M imidazole. The final wash was dialyzed against 20 mM Na_2HPO_4 buffer (pH 8.0) before it was run through a 1.5 × 10 cm Pharmacia Q Sepharose fast flow column (0.7 mL/min). The protein was quantitated at the end of the procedure by the Bradford assay (Bio-Rad kits) with bovine serum albumin as the standard.

For the purification of R38H/H42V hHRP, an additional dialysis step was employed prior to the Ni-NTA agarose column chromatography. The filtered enzyme concentrate was dialyzed overnight against 20 mM Na_2HPO_4 buffer, pH 8.0, containing 500 mM NaCl. During the second dialysis procedure prior to Q Sepharose chromatography, 0.01 M imidazole was added to the 20 mM Na_2HPO_4 buffer, pH 8.0, due to the instability of the protein in the absence of

Table 1: Rates of Compound **I** Formation for HRP and its Mutants (pH 7, 4 °C)

enzyme	$[H_2O_2]$, μM	k, M^{-1} s^{-1}
native HRP	2.5−12.5	3.4×10^7
wt hHRP	2.5−12.5	$(3.6 \pm 0.7) \times 10^7$
R38A	2.5−25.0	$(8.0 \pm 0.5) \times 10^4$
R38H	2.5−40.0	$(1.3 \pm 0.1) \times 10^6$
R38H/H42V	$5-50 \times 10^3$	$(1.6 \pm 0.1) \times 10^3$

either imidazole or high ionic strength (500 mM NaCl). After QFF Sepharose, the enzyme was concentrated using an Amicon system and the final R38H/H42V hHRP preparation was dialyzed overnight against 20 mM Na_2HPO_4 buffer, pH. 8.0, containing 500 mM NaCl.

*Spectroscopic Characterization of Compounds **I** and **II**.* Compound **I** of R38A hHRP was generated by adding 1 equiv of H_2O_2 to the ferric enzyme. Efforts to detect a compound **II** intermediate included adding up to 18 equiv of $K_4Fe(CN)_6$ to compound **I** and allowing compound **I** to decay spontaneously. Efforts were similarly made by static spectroscopic methods to observe compounds **I** and **II** of the R38H and R38H/H42V mutants. However, some of the reaction intermediates formed by the R38A, R38H, and R38H/H42V mutants could only be detected by stopped-flow methods (see below).

*Rate of Compound **I** Formation.* To determine the rate of compound **I** formation by native HRP or the R38A, R38H, and R38H/H42V hHRP mutants, and to detect this intermediate in the case of the R38A mutant, the spectrum was monitored after mixing the enzyme with different amounts of H_2O_2 in an Applied Photophysics model SF.17MV stopped-flow spectrophotometer. The data were analyzed with the program Xscan, (Version 1.00; by P. J. King, Applied Photophysics Ltd., 1995). To follow compound **I** formation under pseudo-first-order conditions, the enzyme (final concentration 0.25 μM) in 100 mM Na_2HPO_4 buffer, pH 7.0, at 4 °C or 25 °C, was treated with excess aqueous H_2O_2 (final concentration 2.5−25.0 μM for R38A, 2.5−40.0 μM for R38H, 5−50 mM for R38H/H42V, and 2.5−12.5 μM for wild-type hHRP or native HRP) (See Table 1.) The data were analyzed using the Pro/Kineticist program (Glint, Version 4.10, by P. J. King and M. Maeder, Applied Photophysics Ltd., Leatherhead, U.K., 1993). The second-order rate constant for compound **I** formation was determined from the slope of the plot of $k_{(obs)}$ versus the H_2O_2 concentration (*26*).

Guaiacol Oxidation. Steady-state kinetic constants were obtained by measuring the initial rates for the oxidation of guaiacol (0.05−10.0 mM) at 25 °C with optimal concentrations of H_2O_2 (see concentrations in Table 2). Different H_2O_2 concentrations were required to optimize product formation while minimizing H_2O_2-dependent enzyme inactivation. The reaction was carried out in 50 mM Na_2HPO_4 buffer at pH 6.0 for native HRP and R38H hHRP, at pH 9.0 for R38A hHRP, and at pH 8.0 for R38H/H42V hHRP. Guaiacol oxidation was monitored at 460 nm, and V_0 was calculated using the absorbance value $\epsilon_{470} = 2.6 \times 10^4$ M^{-1} cm^{-1} (*28*). The apparent k_{cat} and K_m values were estimated from Lineweaver−Burk plots as the arithmetic mean of two independent experiments. To measure the pH dependence of guaiacol oxidation, the following conditions were used: 2 nM native HRP, 40 nM R38A hHRP, 2.5 nM R38H hHRP, or 120−160 nM R38H/H42V hHRP and 5 mM guaiacol and 1.0 mM H_2O_2 in 50 mM Na acetate, Na phosphate, or Tris-HCl buffer at 25 °C.

Table 2: Apparent Kinetic Parameters for Guaiacol Oxidation at 25 °C

enzyme	[E], nM	pH	$[H_2O_2]$, mM	k_{cat}, s^{-1}	K_m, mM	k_{cat}/K_m mM^{-1} s^{-1}
native HRP	2.0	6.0	1.0	420 ± 40	5.8 ± 0.7	72
+ NaCl[a]	2.0	6.0	1.0	660 ± 20	5.0 ± 0.6	132
R38A	40.0	9.0	1.0	41 ± 05	0.6 ± 0.1	68
R38H	2.5	6.0	2.5	200 ± 14	0.5 ± 0.1	400
R38H/H42V + NaCl[a]	119	8.0	10.0	12 ± 1	34 ± 1	0.35

[a] The incubation mixture contained 0.25 mM NaCl.

Table 3: Apparent Kinetic Parameters for ABTS Oxidation at 25 °C

enzyme	$[E]_0$ nM	pH	$[H_2O_2]$, mM	k_{cat}, s^{-1}	K_m, mM	k_{cat}/K_m, mM^{-1} s^{-1}
native HRP	0.2	4.6	10	4100 ± 100	0.80 ± 0.01	5125
+ NaCl[a]	0.2	4.6	10	340 ± 60	0.43 ± 0.02	800
R38A	20.0	4.6	72	660 ± 30	0.40 ± 0.04	1650
R38H	1.3	4.6	20	1400 ± 180	1.6 ± 0.3	875
R38H/H42V + NaCl[a]	57.4	8.0	20	130 ± 12	0.16 ± 0.4	813

[a] The incubation mixture contained 0.25 mM NaCl.

ABTS Oxidation. Apparent steady-state kinetic constants were obtained by measuring the initial rates of oxidation of ABTS (0.02−10.0 mM) at 25 °C with optimal concentrations of H_2O_2 (see Table 3) in 50 mM Na acetate buffer, pH 4.6, except for R38H/H42V for which pH 8.0 was used. Different H_2O_2 concentrations were required to optimize product formation while minimizing H_2O_2-dependent enzyme inactivation. ABTS oxidation was monitored at 414 nm, and V_0 was calculated using $\epsilon_{414} = 3.6 \times 10^4$ M^{-1} cm^{-1} (*28*). The apparent k_{cat} and K_m values were estimated from Lineweaver−Burk plots as the arithmetic mean of three independent determinations. To measure the pH dependence of ABTS oxidation, the following conditions were used: 0.2 nM native HRP, 20 nM R38A hHRP, 1.25 nM R38H hHRP, or 57 nM R38H/H42V hHRP, 10−20 mM ABTS and 10 mM H_2O_2 in 50 mM Na acetate, Na phosphate, or Tris-HCl buffer at 25 °C.

Thioanisole Sulfoxidation. H_2O_2 was added to a concentration of 0.5 mM to 1 mL of a solution at 23 °C of native or mutant HRP and thioanisole in 50 mM Na_2HPO_4 buffer, pH 7.0. For the determination of apparent K_m and k_{cat} values, thioanisole concentrations of 0.1−5.0 mM were used (added as a methanol solution). After a total incubation time of 5 min for R38H or native HRP and 20 s for R38A or R38A/H42V, 5−10 nmol of benzophenone was added as an internal standard, and the solution was extracted with 1 mL of CH_2Cl_2. The extracts were concentrated nearly to dryness, redissolved in 100 μL of HPLC solvent, and filtered using nylon Cameo 3N syringe filters (Micron Separations, Inc.). The residue was analyzed by isocratic HPLC on a Chiralcel OD chiral column (Diacel Chemical Industries, LTD) installed in a Hewlett-Packard model 1040A system equipped with a diode array detector and a Varian 1090 solvent pump system. The HPLC effluent was monitored at 242 nm. The

Table 4: Apparent Kinetic Parameters for Thioanisole Sulfoxidation (23 °C, pH 7, 0.5 mM H_2O_2)

enzyme	$[E]_0$, μM	*S*:*R*	k_{cat}, s^{-1}	K_m, mM	k_{cat}/K_m, mM^{-1} s^{-1}
native HRP	25.0	21:79	0.048	0.6	0.08
R38A[a]	0.6	64:36	9.1 ± 1.0	0.6 ± 0.1	15
R38H	4.6	34:66	0.05 ± 0.01	0.5 ± 0.1	0.1
R38H/H42V	2.5	30:70	33 ± 6	0.3 ± 0.02	110

[a] Numbers were calculated after 20 s, when the enzyme had lost ~70% of its activity.

products were eluted with hexane/2-propanol (8:2) at a flow rate of 0.5 mL min^{-1}. The retention times for the (*S*)- and (*R*)-isomers of methyl phenyl sulfoxide were 12.6 and 14.6 min, respectively. A standard curve for the products was constructed by injecting known amounts of methyl phenyl sulfoxide.

To test the linearity of product formation as a function of time, 0.5-mL incubations were carried out containing 0.5 mM H_2O_2, 2.0 mM thioanisole, and different amounts of native or mutant hHRP (see Table 4) in 50 mM Na_2HPO_4 buffer, pH 7.0. Reactions were stopped at various time points and analyzed as described above. The reaction was linear for 3−5 min for native and R38H hHRP but not for R38A and R38A/H42V hHRP (see Results).

Styrene Epoxidation. H_2O_2 was added to a final concentration of 15 mM to 0.5 mL of a solution at 23 °C of native or mutant HRP and styrene (added as a methanol solution) in 50 mM Na_2HPO_4 buffer, pH 7.0. For the determination of apparent K_m and k_{cat} values, 0.5−5.0 mM styrene concentrations were used. After a total incubation time of 60 min, the solution was extracted with 1 mL of CH_2Cl_2, extracts were concentrated to 10−30 μL under a stream of argon or N_2, and the concentrate was analyzed on a 0.25 mm × 30 m DB-1 column in a Hewlett-Packard 5890 series II GC system. The column was programmed to run at 80 °C for 17 min and then to rise to 200 °C at 15° min^{-1}, where it remained for 1 min before recycling. The injection and detector temperatures were 200 and 250 °C, respectively. The retention times with a head column pressure of 15 psi were the following: styrene, 5.73 min; benzaldehyde (BA), 6.61 min; phenylacetaldehyde (PAA), 7.97 min; and styrene oxide (SO), 8.48 min. Standard curves for the products were constructed by similarly analyzing known amounts of the authentic compounds. To calculate the percentages of the products formed, the total amounts of the substrate and products calculated from the peak areas using the appropriate coefficients for each compound were considered as 100% of the material.

To test the linearity of product formation with time, 0.5-mL incubations were carried out containing 15 mM H_2O_2, 5 mM styrene, and different amounts of native or mutant HRP (see Table 5) in 50 mM sodium phosphate buffer, pH 7.0. Reactions were stopped at various time points and analyzed as described above. The reaction was linear for at least 60 min.

RESULTS

Construction, Expression, and Purification of R38A, R38H, and R38H/H42V hHRP. The R38A, R38H, and R38H/H42V mutants of hHRP were constructed by cassette mutagenesis and were expressed in *T. ni* cells. The three mutants, and the wild-type enzyme (*26*), have a polyhistidine tag at the amino terminus that facilitates their purification by Ni(II)-NTA affinity chromatography. The yields of the pure proteins were 8−15 mg L^{-1} of culture. The purities of the isolated proteins were high, as judged by the presence of single bands on SDS−PAGE (not shown). The R_z values of the purified proteins were 3.0 for wild-type, 2.6 for R38A, 2.5 for R38H, and 1.3 for R38H/H42V hHRP. Upon reconstitution of R38H/H42V hHRP with heme followed by passage through a bovine serum albumin-Sepharose column to remove excess heme, the R_z for the protein only increased slightly to a value of 1.6. The R38H/H42V enzyme was therefore used as isolated. The R38H/H42V double mutant was chosen for study instead of the R38H/H42A mutant because the latter, which was also prepared, was too unstable for the present studies.

Table 5: Apparent Kinetic Parameters for Styrene Epoxidation (23 °C, pH 7, 15 mM H_2O_2)

enzyme	$[E]_0$, μM	BA:PAA:SO[a]	k_{cat}, s^{-1}	K_m, mM	k_{cat}/K_m, mM^{-1} s^{-1}
native HRP	98.0	22:36:42	0.0001	0.3	0.0003
R38A	11.4	10:54:36	0.023 ± 0.002	3.1 ± 1.4	0.0074
R38H	9.2	50:12:38	0.0037 ± 0.0002	1.9 ± 0.7	0.0019
R38H/H42V	2.5	10:61:29	0.0031 ± 0.0001	0.4 ± 0.2	0.0078

[a] Abbreviations: BA, benzaldehyde; PAA, phenylacetic acid; SO, styrene oxide.

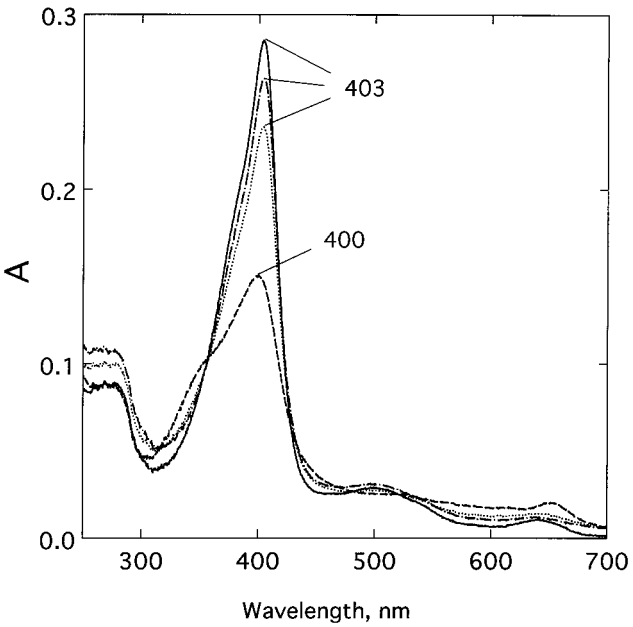

FIGURE 2: Reaction of R38A hHRP with 1 equiv of H_2O_2 at pH 7.0, 25 °C. The same result is obtained with 1 equiv of H_2O_2 by stopped-flow spectroscopy (not shown). The spectra are of the ferric R38A enzyme (−); compound **I** obtained by addition of 1 equiv of H_2O_2 to the enzyme (− − −); and the enzyme after addition to compound **I** of 0.5 (···) or 1.0 (− · −) eq of $K_4Fe(CN)_6$.

Reaction of R38A with H_2O_2. Reaction of R38A hHRP, which has a Soret maximum at 403 nm, with 1 equiv of H_2O_2 produces a typical compound **I** spectrum, with no shift of the Soret band from its position in the ferric enzyme, a 2-fold decrease in the Soret intensity, and a flattened α/β band region (Figure 2). Addition of 1 equiv of $K_4Fe(CN)_6$ to compound **I** leads to recovery of the resting ferric enzyme

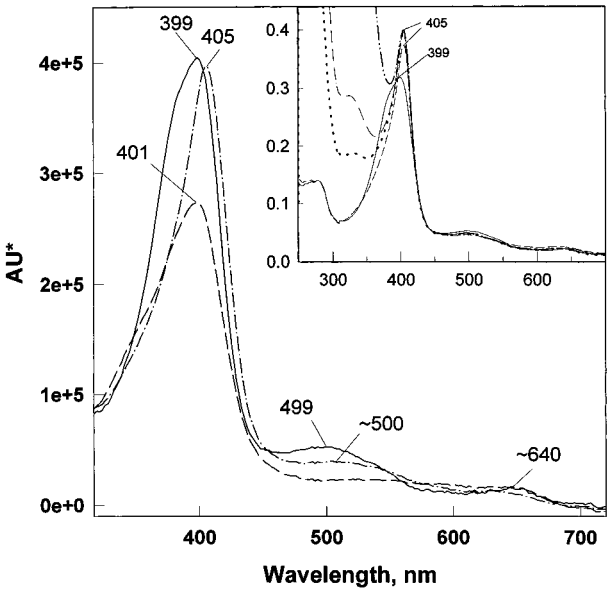

FIGURE 3: Characterization by stopped-flow spectroscopy of the reaction of R38H hHRP with 10 equiv of H_2O_2 at pH 7.0, 4 °C. The spectra are for the intermediates calculated by the computer for the reaction A → B → C: ferric enzyme (−), compound **I** obtained ~1 s after mixing the ferric enzyme and H_2O_2 (− − −), and the spectrum obtained ~10 s after mixing the enzyme with H_2O_2 (− · −). The inset, determined at 25 °C, shows the spectrum of ferric R38H (−), the spectrum obtained by addition of 1 equiv of H_2O_2 (− − −), and the spectrum obtained by further addition of 1.0 (···), 2.0 (− · −), and 18 (− · · −) equiv of $K_4Fe(CN)_6$.

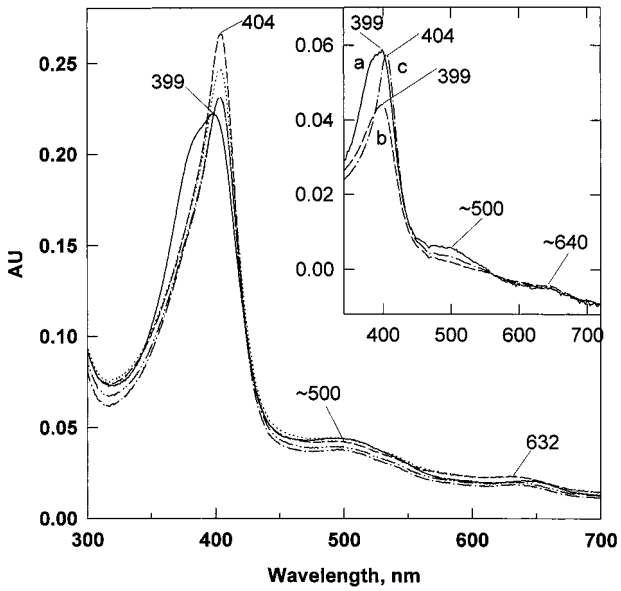

FIGURE 4: Static spectroscopic characterization of the reaction of R38H/H42V hHRP with 1 and 100 equiv (inset) of H_2O_2 at pH 7.0. In the main panel is shown the spectrum of ferric R38H/H42V hHRP (−) and the spectra obtained at 23 °C after addition to the ferric enzyme of 1 equiv of H_2O_2 (− − −) followed by 1 (···), 2 (− · −), and 100 equiv (− · · −) of $K_4Fe(CN)_6$. The spectra in the inset are for transient intermediates detected at 4 °C by stopped-flow spectroscopy: ferric enzyme (−), compound **I** obtained ~1 s after mixing with 100 eq H_2O_2 (− − −), and the species obtained ~10 s after mixing with 100 equiv of H_2O_2 (− · −).

(Figure 2) without observation of a compound **II**-like spectrum. compound **II** is normally characterized by approximately a 10-nm red-shift of the Soret band with a recovery of Soret band intensity. Compound **II** is also not observed when the R38A compound **I** obtained with 1 equiv of H_2O_2 is allowed to decay spontaneously over 30−90 min to the ferric state (not shown). A compound **II** species is also not observed by stopped-flow spectroscopy if 1 equiv of H_2O_2 is used to generate compound **I**, although a species with $\lambda_{max} = 408$ nm (possibly compound **III**) is detected if a 10-fold excess of H_2O_2 is employed in the reaction. Compound **II** of the R38L HRP mutant has been reported to be very short-lived (*17*).

Reaction of R38H with H_2O_2. Addition of from 1 to 100 equiv of H_2O_2 to R38H hHRP, which has an asymmetric Soret maximum at 399 nm, only produces a sharp and slightly more intense Soret band at 405 nm without the 380 nm shoulder (Figure 3). Addition of up to 18 equiv of $K_4Fe(CN)_6$ to this species causes little change in its spectrum (Figure 3, inset). This species, which is clearly not a compound **I** intermediate, appears to be a form of the ferric protein with an altered iron coordination state. However, if the reaction is monitored by stopped-flow techniques, the transient formation of a typical compound **I** spectrum can be observed after the addition of 2.5 or more equiv of H_2O_2 (Figure 3). Thus, the Soret intensity decreases to half of its original value with a slight shift of λ_{max} from 399 to 401 nm (Figure 3). At pH 7.0 and 4 °C, this compound **I** species is not stable and spontaneously decays within 0.4 s to the species with $\lambda_{max} = 405$ nm and very broad α/β bands at ~640 and ~500 nm, respectively.

Reaction of R38H/H42V with H_2O_2. As shown for R38H hHRP, the R38H/H42V hHRP mutant, which also has an asymmetric Soret band at 399 nm, reacts with 1 equiv of H_2O_2 to produce a spectrum with a more intense Soret maximum at $\lambda_{max} = 404$ nm and α/β bands at 632 and ~500 nm, respectively (Figure 4). Addition of up to 100 equiv of $K_4Fe(CN)_6$ to this species only slightly decreases the intensity of the 404-nm peak (Figure 4). Neither a compound **I** nor a compound **II** intermediate is detected by this static spectroscopic method. However, as found for the R38H mutant, both of these intermediates can be detected at 4 °C by stopped-flow spectroscopy. Reaction of R38H/H42V hHRP with up to a 100-fold excess of H_2O_2 produces during the first 0.5−2.0 s a sharper Soret band with an unchanged maximum at 399 nm but approximately $^1/_2$ of the starting intensity (Figure 4, inset). During the subsequent 5−10 s, the Soret absorbance increases and shifts to 404 nm to give the final spectrum. Further incubation leads to a gradual decrease in the Soret absorbance due to prosthetic group degradation.

*Rate of Compound **I** Formation.* The rate of compound **I** formation was determined by monitoring the absorption spectrum between 350 and 750 nm after adding varying amounts of H_2O_2 to the ferric enzyme. The value of $k_{(obs)}$ was calculated by a computer algorithm as the rate constant for formation of a new species (compound **I**) from the ferric enzyme. This was done by fitting the calculated kinetic curve to the scan of the actual Soret band λ_{max} and by matching the calculated final spectrum of the new species to the real final spectrum of compound **I**. As the response time of the instrument limits the accuracy of the rate determined at 25 °C for compound **I** formation with the native enzyme, the rates for the mutant enzymes were compared with those for the native and wild-type proteins at 4 °C. At this temperature, the rate constants for compound

I formation for the R38A, R38H, and R38H/H42V enzymes are $(8.0 \pm 0.5) \times 10^4$, $(1.3 \pm 0.1) \times 10^6$, and $(1.6 \pm 0.1) \times 10^3$ M^{-1} s^{-1}, respectively (Table 1). These values are approximately 450-, 28-, and 21000-fold lower, respectively, than those for the native and wild-type enzymes.

Steady-State Kinetics of Guaiacol and ABTS Oxidation. The R38A, R38H, and R38H/H42V hHRP mutants catalyze the peroxidation of guaiacol and ABTS. The pH optimum for guaiacol oxidation by the R38H mutant is 6.8, a value similar to that for native HRP; however, the pH profile for the R38A mutant is more narrow, and the maximum is shifted to 8.6−9.5. At pH values <7.0, R38A hHRP has very low guaiacol oxidizing activity. The R38H/H42V hHRP pH profile for guaiacol oxidation is also narrow and has a maximum at pH 7−8: at pH 2−5 the enzyme has very low guaiacol oxidation activity.

The kinetics of guaiacol oxidation by native HRP and the R38A, R38H, and R38H/H42V mutants have been examined to evaluate the role of Arg38 in peroxidase catalysis. The apparent K_m values for guaiacol oxidation by R38A, R38H, and R38H/H42V hHRP are 0.6, 0.5, and 34 mM, respectively. These values are to be compared with an apparent K_m of 5.8 mM for the native enzyme (Table 2). The apparent k_{cat} values for guaiacol oxidation by the R38A, R38H, and R38H/H42V mutants are 41, 200, and 12 s^{-1}, respectively. The corresponding value for native HRP is 420 s^{-1}. The activities of the R38A and R38H/H42V mutants, as judged from their relative k_{cat} values, are therefore 10- and 55-fold lower than that of the native enzyme, whereas the R38H mutant is only 2-fold less active than native HRP. The guaiacol oxidation efficiency (i.e., apparent k_{cat}/K_m) of R38A hHRP is almost the same as that for the native enzyme, that of R38H hHRP is 6-fold higher, and that of the R38H/H42V mutant is 380-fold lower if it is compared to native HRP in the presence of a similar high salt concentration. The activities of R38H/H42V hHRP were measured in the presence of a high salt concentration because it is unstable in the absence of either imidazole or a high salt concentration. The kinetic studies were carried out for each enzyme near its pH optimum, and the pH optima of the enzymes differ (Table 2).

The pH optima for ABTS oxidation by the R38A, R38H, and R38H/H42V, and native proteins are 5.2, 4.6, 8.0, and 4.6, respectively. The pH profiles for the oxidation of ABTS show that R38H hHRP has little or no activity at pH > 6, that R38A hHRP is active up to pH 8, and that R38H/H42V hHRP has little activity at pH values <6. Kinetic studies of ABTS oxidation for the native and single mutants were carried out at pH 4.6 and for the double mutant at pH 8.0 (Table 3). The concentrations of H_2O_2 used in these studies differed and were optimal for each enzyme.

The apparent K_m values for ABTS oxidation by the R38A, R38H, and R38H/H42V enzymes are 0.4, 1.6, and 0.16 mM, respectively (Table 3). These values are to be compared with an apparent K_m of 0.8 mM (0.43 mM at high salt concentration) for native HRP. The apparent k_{cat} values for ABTS oxidation by R38A, R38H, and R38H/H42V hHRP are 660, 1400, and 130 s^{-1}, respectively, and the corresponding value for native HRP is 4100 s^{-1} (340 s^{-1} at high salt concentration) (Table 3). Thus, the activities of the R38A, R38H, and R38H/H42V mutants, as judged by their k_{cat} values, are approximately 6-, 3-, and 32-fold lower, respectively, than that of the native enzyme, and their efficiencies, as given by their apparent k_{cat}/K_m values, are ~3-, 6-, and 12-fold lower, respectively. If the R38H/H42V data is compared against the wild-type enzyme under high salt conditions, the apparent k_{cat} value is only 2.6-fold lower, and the efficiency is essentially unchanged.

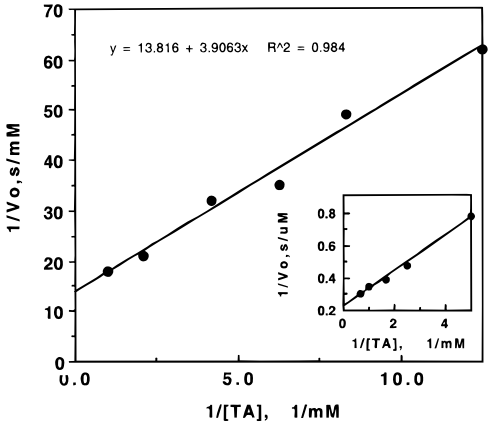

FIGURE 5: Lineweaver−Burke plots for the oxidation of thioanisole by the R38H/H42V double mutant and (inset) the R38A mutant. TA stands for thioanisole. Similar plots are obtained for the oxidation of styrene.

Peroxygenase Reactions. The time course for the oxidation of thioanisole by R38H and R38H/H42V hHRP is linear for at least 5 min and 20 s, respectively (Figure 5). However, thioanisole sulfoxidation by the R38A mutant is nonlinear (the first two time points were taken at 5 and 10 s) even at a low (57 nM) concentration of the enzyme due to rapid inactivation by H_2O_2. Michaelis−Menten parameters for thioanisole oxidation were calculated for the three mutants, but the calculated kinetic parameters for R38A hHRP may underestimate the true values due to enzyme inactivation (Table 4). The apparent kinetic parameters for R38A, R38H, and R38H/H42V are K_m = 0.6, 0.5, and 0.3 mM and k_{cat} = 9.1, 0.05, and 33 s^{-1}, respectively. These values are to be compared with an apparent K_m of 0.6 mM and k_{cat} of 0.048 s^{-1} for native HRP. The reaction efficiencies of the R38A, R38H, R38H/H42V, and native hHRP, as judged from their apparent k_{cat}/K_m values, are 15, 0.1, 110, and 0.08 mM^{-1} s^{-1}, respectively. Thus, R38A and R38H/H42V hHRP are at least 190- and 1400-fold more efficient in thioanisole oxidation, respectively, than the native enzyme. The R38H mutant has the same thioanisole sulfoxidation activity and efficiency as native HRP. R38H and R38H/H42V hHRP closely resemble native HRP in that they produce more of the (*R*)- than (*S*)-sulfoxide enantiomer, whereas the R38A mutant produces more of the (*S*)-isomer (Table 4).

Styrene oxidation by HRP produces styrene oxide (SO) and phenylacetaldehyde (PAA) (*28*). A third product, benzaldehyde (BA), is also formed but appears to be generated by a nonenzymatic mechanism. All four enzymes produce roughly similar percentages of styrene oxide, but the proportion of PAA differs. R38A and R38A/H42V hHRP produce more, and R38H produces less PAA than the native enzyme (Table 5). As a nonenzymatic product, benzaldehyde has not been taken into consideration in calculating V_0. The apparent kinetic parameters for styrene epoxidation by the R38A, R38H, and R38H/H42V mutants are K_m = 3.1, 1.9, and 0.4 mM, and k_{cat} = 0.023, 0.0037,

and 0.0031 s^{-1}, respectively. The corresponding apparent values for the native enzyme are $K_m = 0.3$ mM and $K_{cat} = 0.0001$ s^{-1}. The efficiencies of the R38A, R38H, R38H/H42V, and native enzymes, as given by the apparent k_{cat}/K_m values, are 0.0074, 0.0019, 0.0078, and 0.0003 mM^{-1} s^{-1}, respectively. Thus, the R38A, R38H, and R38H/H42V mutants are 230-, 37-, and 31-fold more active, and 25-, 6-, and 26-fold more efficient, respectively, in styrene oxidation than the native enzyme.

DISCUSSION

The R38A, R38H, and R38H/H42V hHRP mutants were constructed and examined to determine whether a histidine can replace Arg38 in the catalytic mechanism and, more importantly, whether replacement of Arg38 by a histidine can compensate in peroxidative and peroxygenative catalysis for simultaneous replacement of His42 by an alanine or a valine. This choice of mutations was based on the premise that the low peroxygenase activity of HRP is due to steric interference with the interaction of the substrate with the ferryl oxygen (*2*, *23*, *24*). Examination of the crystal structure of peanut peroxidase, which is closely related to HRP, and of other available peroxidase crystal structures indicates that the key residues in HRP that limit interaction of the substrate with the ferryl oxygen are Phe41, His42, and Arg38. His42 is particularly critical in this regard, as it sits in the center of the access channel over the heme iron atom (Figure 1). Thus, mutations that reduce the bulk of these residues should make the iron more available and thus improve the peroxygenase activity of the enzyme. Unfortunately, His42 and Arg38 are critical catalytic residues, and their replacement by neutral residues slows down the catalytic activation of H_2O_2 and consequently the rate of enzyme turnover. Thus, the rate of formation of compound **I** decreases from 0.89×10^7 M^{-1} s^{-1} to 1.94×10^1 M^{-1} s^{-1} upon mutation of His42 to an alanine (*25*) and to 1.1×10^4 M^{-1} s^{-1} upon mutation of Arg38 to a leucine (*20*). Despite the drastic decrease in the rate of compound **I** formation caused by the H42A mutation, which is reflected in a decreased rate of guaiacol peroxidation, the apparent k_{cat} values for thioanisole sulfoxidation and particularly styrene epoxidation for the mutant (0.03 and 0.007 s^{-1}, respectively) are as high as or higher than for the wild-type enzyme (0.05 and 1×10^{-6} s^{-1}, respectively) (*26*). Mutation of Phe41 to an alanine does not significantly alter the rate of compound **I** formation but increases the rates of thioanisole sulfoxidation and styrene epoxidation (*25*). However, Phe41 is placed in the active site (Figure 1) in such a way that its replacement with smaller residues does not open up access to the iron to the same extent as does mutation of His42. This finding is in accord with the observation that the F41A mutation does not improve styrene epoxidation activity as much as the H42A mutation despite the difference of $\sim 10^6$ in their rates of compound **I** formation (*25*).

In an effort to preserve rapid compound **I** formation while decreasing the size of the residue at position 42, we demonstrated earlier that complementation of the H42A mutation with an F41H mutation produces a peroxygenase catalyst more effective than the H42A mutant (*26*). The rate of compound **I** formation with the F41H/H42A double mutant is 3×10^4 M^{-1} s^{-1}, approximately 10^3-fold faster than that of the H42A mutant. Furthermore, the apparent k_{cat} values for guaiacol (1.8 s^{-1}) and ABTS (100 s^{-1}) peroxidation by the double mutant are considerably higher than the corresponding values of 0.12 and 0.41 s^{-1} for H42A hHRP. Most significantly, a real improvement was observed in the thioanisole sulfoxidation (5.3 s^{-1}) and styrene epoxidation (0.024 s^{-1}) rates (*26*).

The R38A, R38H, and R38H/H42V mutants, obtained in high purity and yield by heterologous expression in a baculovirus/insect cell system, exhibit differences in their Soret maxima suggestive of differences in iron coordination state. The spectrum of the ferric R38A mutant, with a sharp Soret maximum at 404 nm, differs only slightly from that of the wild-type enzyme and the previously reported R38G mutant (*29*). In contrast, the Soret bands of the R38H and R38H/H42V mutants have maxima at 399 nm and are relatively broad due to the presence a shoulder at ~380 nm. These spectra resemble those reported for the R38L mutant, which was shown by resonance Raman spectroscopy to have a predominantly pentacoordinate, high-spin iron configuration (*29*). These spectra suggest that the R38A, R38H, and R38H/H42V mutants have essentially intact active sites.

The reaction of H_2O_2 with the R38A, R38H, and R38H/H42V hHRP, as indicated by a 1.5−2-fold decrease in Soret band intensity with no more than a minor shift in its position, in each instance produces a detectable compound **I** species (Figures 2−4). In the case of the R38A mutant, compound **I** is observed if 1 equiv of H_2O_2 is simply added to the protein (Figure 2, inset), but compound **I** is not observed with the R38H and R38H/H42V mutants except by stopped-flow methods. The only change observed by static spectroscopic methods with these proteins upon addition of 1 or several equiv of H_2O_2 to these proteins is a sharpening and ~5-nm red-shift of their Soret bands with a slight increase in molar absorbance. These spectra correspond to modified ferric proteins because the spectra are little altered by the addition of ferricyanide. The nature of the modification caused by reaction with H_2O_2 is unclear, but the result is a change in the coordination state of the iron. However, if the R38H and R38H/H42V reactions are monitored by stopped-flow methods at very short time periods after H_2O_2 is added, spectra characteristic of compound **I** species are transiently observed (Figures 3 and 4).

Reduction of the easily observed R38A compound **I** to the ferric state proceeds without the detectable formation of compound **II** whether the reduction is promoted by $K_4Fe(CN)_6$ or simply allowed to occur with time (Figure 2). However, a compound **II**-like species can be detected by stopped-flow spectroscopy following the transient formation of compound **I**-like species with the R38H and, less convincingly, with the R38H/H42V mutants (Figures 3 and 4). The properties of the hypervalent ferryl states of R38A hHRP resemble those reported previously for the R38L mutant (*20*), in that it gives a stable compound **I** species but a very unstable or undetectable compound **II** species. In the case of R38H and R38H/H42V hHRP, both compounds **I** and **II** are sufficiently unstable that they are not detected except by stopped-flow methods. This instability is clearly linked to the R38H mutation because compound **I** is readily observed with the H42A and H42V mutants (*25*).

The rates of compound **I** formation are impaired when Arg38 is replaced by a neutral amino acid. Replacement of Arg38 by a noncatalytic alanine results in a 450-fold decrease

in the rate of compound **I** formation. This is comparable to the decrease of ~10^3 previously observed with the R38L mutant (*20*). Stopped-flow studies of the R38L mutant resulted in observation of a transient species with an absorption spectrum slightly different from that of the ferric enzyme prior to the formation of compound **I**. This transient spectrum was tentatively attributed to the ferric peroxo (FeOOH) complex, in which case cleavage of the peroxo complex is the rate-limiting step in the mutant (*20*). Spectra of the reaction of the R38A mutant with H_2O_2 taken at very short reaction times also exhibit small changes that differ from those that lead to compound **I** formation, but the changes are not the same as those reported for the R38L mutant. In the absence of more definitive data on the nature of the transient species obtained with either the R38L or R38A mutant, we cannot conclude that the ferric peroxo complex is observed in our experiments.

In contrast, compound **I** formation with R38H hHRP was only 28-fold slower than with wild-type hHRP (Table 1). Thus, a histidine at position 38 substitutes to some extent for Arg38 in the catalytic mechanism but not in stabilization of compound **I**. Rodriguez-Lopez et al. (*20*) have proposed that Arg38 promotes compound **I** formation by (a) facilitating proton transfer to His42 and thus assisting binding of the peroxide anion to the iron and (b) stabilizing the transition state for heterolytic oxygen−oxygen bond cleavage. Our earlier demonstration that exogenous imidazoles (*16*), or an imidazole substituted for Phe41 (*26*), partially rescue the catalytic activity of the His42 mutant by facilitating binding of the peroxide anion to the iron suggest that the histidine at position 38 may also fulfill this function of Arg38. It is not possible at this point to determine whether the histidine substitutes to some extent for Arg38 in stabilizing the transition state for peroxide bond cleavage.

The rate for compound **I** formation in the R38H/H42V mutant is 1.6×10^3 M^{-1} s^{-1}, approximately 21000-fold slower than for wild-type hHRP. On the other hand, the rate of compound **I** formation for the H42V mutant is 1.0×10^1 M^{-1} s^{-1}, a rate approximately 10^6-fold lower than for the wild-type (*25*). Thus, replacement of Arg38 by a histidine improves the rate of compound **I** formation of the H42V mutant by a factor of approximately 150, presumably because the histidine, even if not optimally located, is a more versatile catalytic residue than the arginine.

Key results emerge from comparisons of the effects of the mutations on the peroxidation of guaiacol and ABTS and on the peroxygenation of thioanisole and styrene. Replacement of Arg38 by an alanine decreases the apparent k_{cat} values for the oxidation of guaiacol and ABTS by a factor of <10, a value considerably smaller than the decrease of ~450 in the rate of compound **I** formation. Replacement of Arg38 by a histidine decreases the two peroxidation rates by a factor of <3, again an effect 10-fold lower than that of the mutation on compound **I** formation. The same is true for the R38H/H42V mutation, which causes a decrease in the peroxidative rates much smaller than that in compound **I** formation (Tables 1 and 2). The smaller effect of the R38H than R38A mutation on peroxidative catalysis indicates that the histidine can partially substitute for the arginine in the catalytic mechanism. The effects of the R38A, R38H, and R38H/H42V mutations on peroxidative catalysis which are much smaller than those on compound **I** formation agree with the conclusion that compound **I** formation is not the only rate-limiting step in the reaction.

In contrast to peroxidative catalysis, which is modestly impaired by mutations of the catalytic residues His42 and Arg38, peroxygenative catalysis is actually improved by the same mutations (Tables 4 and 5). Thus, the R38A mutation increases the apparent k_{cat} values for thioanisole sulfoxidation and styrene epoxidation 182- and 660-fold, and the R38H/H42V-coupled mutations increase the same parameters 230- and 31-fold. In the R38A mutant, the relatively large Arg38 group is replaced by a small but catalytically incompetent alanine residue. In the R38H/H42V double mutant, Arg38 is replaced by a large histidine residue, but His42 is replaced by a relatively small valine. Together, these mutations increase the size of the cavity and, therefore, access to the active site. If Arg38 is replaced by a comparably large histidine residue without simultaneous changes at the His42 site, the rate of thioanisole sulfoxidation is not altered and that of styrene epoxidation is increased 37-fold. The increases seen with the R38A and R38H/H42V mutations must be placed in the context of the 450- and 21000-fold decreases in compound **I** formation. These results, together with the earlier results obtained with the F41A and H42A mutations (*25*, *26*, *28*), indicate that steric access to the activated oxygen species exerts a major control on the rate of the peroxygenase reactions. Furthermore, the collective results indicate that much better peroxygenase catalysts can be constructed by increasing that access, even if the modifications impair the catalytic machinery involved in formation and stabilization of the activated species.

Although higher intrinsic peroxygenase activities are achieved with the R38A and R38H/H42V mutations, the mutations also decrease the stability of the ferryl species and lead to accelerated catalysis-dependent inactivation of the enzyme. Studies with cytochrome *c* peroxidase have indicated that Arg48, the residue equivalent to Arg38 in HRP, is important not so much for compound **I** formation as for stabilization of the compound **I** ferryl species (*15*, *30*). The stabilization may include an electrostatic component but also involves a hydrogen bond to the ferryl oxygen (*31*−*33*). Arg38 appears to have a more significant role in compound **I** formation in HRP; however, the present results show that it is also critical for stabilization of the ferryl species, presumably as the result of both static and hydrogen bonding interactions. A further requirement may be that the residue at position 38 needs to be resistant to reaction with the activated oxygen species, a possible basis for the very poor stability of the R38H and R38H/H42V hHRP compound **I** species. The construction of optimal peroxygenase catalysts based on the HRP skeleton thus requires the elaboration of mutations that increase access to the active site but preserve stabilization of the reactive ferryl species even if they cause a decrease in the rate of compound **I** formation.

REFERENCES

1. Dunford, H. B. (1991) in *Peroxidases in Chemistry and Biology* (Everse, J., Everse, K. E., and Grisham, M. B., Eds.) Vol. 2, pp 1−24, CRC Press, Boca Raton.
2. Ortiz de Montellano, P. R. (1992) *Annu. Rev. Pharmacol. Toxicol. 32*, 89−107.
3. Dolphin, D., Forman, A., Borg, D. C., Fajer, J., and Felton, R. H. (1974) *Proc. Natl. Acad. Sci. U.S.A. 68*, 614−618.

4. Baek, H. K., and Van Wart, H. E. (1992) *J. Am. Chem. Soc. 114*, 718−725.
5. Sivaraja, M., Goodin, D. B., Smith, M., and Hoffman, B. M. (1989) *Science 245*, 738−740.
6. Dunford, H. B., and Stillman, J. S. (1976) *Coord. Chem. Rev. 19*, 187−251.
7. Finzel, B. C., Poulos, T. L., and Kraut, J. (1984) *J. Biol. Chem. 259*, 13027−13036.
8. Poulos, T. L., Edwards, S. L., Wariishi, H., and Gold, M. H. (1993) *J. Biol. Chem. 268*, 4429−4440.
9. Sundaramoorthy, M., Kishi, K., Gold, M. H., and Poulos, T. L. (1994) *J. Biol. Chem. 269*, 32759−39.
10. Kunishima, N., Fukuyama, K., Matsubara, H., Hatanaka, H., Shibano, Y., and Amachi, T. (1994) *J. Mol. Biol. 235*, 331−344.
11. Schuller, D. J., Ban, N., van Huystee, R. B., McPherson, A., and Poulos, T. L. (1996) *Structure 4*, 311−321.
12. Patterson, W. R., and Poulos, T. L. (1995) *Biochemistry 34*, 4331−4341.
13. Poulos, T. L., and Kraut, J. (1980) *J. Biol. Chem. 255*, 8199−8205.
14. Erman, J. E., Vitello, L. B., Miller, M. A., Shaw, A., Brown, K. A., and Kraut, J. (1993) *Biochemistry 32*, 9798−9806.
15. Vitello, L. B., Erman, J. E., Miller, M. A., Wang, J., and Kraut, J. (1993) *Biochemistry 32*, 9807−9818.
16. Newmyer, S. L., and Ortiz de Montellano, P. R. (1996) *J. Biol. Chem. 271*, 14891−14896.
17. Rodriguez-Lopez, J. N., Smith, A. T., and Thorneley, R. N. F. (1996) *J. Biol. Chem. 271*, 4023−4030.
18. Sanders, S. A., Bray, R. C., and Smith, A. T. (1994) *Eur. J. Biochem. 224*, 1029−1037.
19. Smulevich, G., Paoli, M., Burke, J. F., Sanders, S. A., Thorneley, R. N. F., and Smith, A. T. (1994) *Biochemistry 33*, 7398−7407.
20. Rodriguez-Lopez, J. N., Smith, A. T., and Thorneley, R. N. F. (1996) *J. Biol. Inorg. Chem. 1*, 136−142.
21. Kobayashi, S., Nakano, M., Goto, T., Kimura, T., and Schaap, A. P. (1986) *Biochem. Biophys. Res. Commun. 135*, 166−71.
22. Doerge, D. R., Cooray, N. M., and Brewster, M. E. (1991) *Biochemistry 30*, 8960−8964.
23. Ortiz de Montellano, P. R. (1987) *Acc. Chem. Res. 20*, 289−294.
24. Ator, M., and Ortiz de Montellano, P. R. (1987) *J. Biol. Chem. 262*, 1542−1551.
25. Newmyer, S. L., and Ortiz de Montellano, P. R. (1995) *J. Biol. Chem. 270*, 19430−19438.
26. Savenkova, M. I., Newmyer, S. L., and Ortiz de Montellano, P. R. (1996) *J. Biol. Chem. 271*, 24598−24603.
27. Nelson, D. P., and Kiesow, L. A. (1972) *Anal. Biochem. 49*, 474−478.
28. Ozaki, S., and Ortiz de Montellano, P. R. (1995) *J. Am. Chem. Soc. 117*, 7056−7064.
29. Howes, B. D., Rodriguez-Lopez, J. N., Smith, A. T., and Smulevich, G. (1997) *Biochemistry 36*, 1532−1543.
30. Erman, J. E., Vitello, L. B., Miller, M. A., and Kraut, J. (1992) *J. Am. Chem. Soc. 114*, 6592−6593.
31. Edwards, S. L., and Poulos, T. L. (1990) *J. Biol. Chem. 265*, 2588−2595.
32. Fülop, V., Phiazckerley, R. P., Soltis, S. M., Clifton, I. J., Wakatsuki, S., Erman, J., Hajdu, J., and Edwards, S. L. (1994) *Structure 2*, 201−208.
33. Bujons, J., Dikiy, A., Ferrer, J. C., Banci, L., and Mauk, A. G. (1997) *Eur. J. Biochem. 243*, 72−84.

BI9725780